



Molecular Simulation of Shocked Materials Using Reaction Ensemble Monte Carlo: Part II. Application to Nitric Oxide Decomposition

by John K. Brennan and Betsy M. Rice

ARL-TR-3984

November 2006

NOTICES

Disclaimers

The findings in this report are not to be construed as an official Department of the Army position unless so designated by other authorized documents.

Citation of manufacturer's or trade names does not constitute an official endorsement or approval of the use thereof.

Destroy this report when it is no longer needed. Do not return it to the originator.

Army Research Laboratory

Aberdeen Proving Ground, MD 21005-5066

ARL-TR-3984**November 2006**

Molecular Simulation of Shocked Materials Using Reaction Ensemble Monte Carlo: Part II. Application to Nitric Oxide Decomposition

John K. Brennan and Betsy M. Rice
Weapons and Materials Research Directorate, ARL

REPORT DOCUMENTATION PAGE				Form Approved OMB No. 0704-0188	
Public reporting burden for this collection of information is estimated to average 1 hour per response, including the time for reviewing instructions, searching existing data sources, gathering and maintaining the data needed, and completing and reviewing the collection information. Send comments regarding this burden estimate or any other aspect of this collection of information, including suggestions for reducing the burden, to Department of Defense, Washington Headquarters Services, Directorate for Information Operations and Reports (0704-0188), 1215 Jefferson Davis Highway, Suite 1204, Arlington, VA 22202-4302. Respondents should be aware that notwithstanding any other provision of law, no person shall be subject to any penalty for failing to comply with a collection of information if it does not display a currently valid OMB control number. PLEASE DO NOT RETURN YOUR FORM TO THE ABOVE ADDRESS.					
1. REPORT DATE (DD-MM-YYYY) November 2006		2. REPORT TYPE Final		3. DATES COVERED (From - To) June 2005–September 2005	
4. TITLE AND SUBTITLE Molecular Simulation of Shocked Materials Using Reaction Ensemble Monte Carlo: Part II. Application to Nitric Oxide Decomposition				5a. CONTRACT NUMBER	
				5b. GRANT NUMBER	
				5c. PROGRAM ELEMENT NUMBER	
6. AUTHOR(S) John K. Brennan and Betsy M. Rice				5d. PROJECT NUMBER H4311	
				5e. TASK NUMBER	
				5f. WORK UNIT NUMBER	
7. PERFORMING ORGANIZATION NAME(S) AND ADDRESS(ES) U.S. Army Research Laboratory ATTN: AMSRD-ARL-WM-BD Aberdeen Proving Ground, MD 21005-5066				8. PERFORMING ORGANIZATION REPORT NUMBER ARL-TR-3984	
9. SPONSORING/MONITORING AGENCY NAME(S) AND ADDRESS(ES)				10. SPONSOR/MONITOR'S ACRONYM(S)	
				11. SPONSOR/MONITOR'S REPORT NUMBER(S)	
12. DISTRIBUTION/AVAILABILITY STATEMENT Approved for public release; distribution is unlimited.					
13. SUPPLEMENTARY NOTES					
14. ABSTRACT This is the second of two reports in which we demonstrate the applicability of the Reaction Ensemble Monte Carlo (RxMC) simulation method for calculating the shock Hugoniot properties of a material. In the first part of this series, we illustrated the methodology on shocked liquid N ₂ , where we found excellent agreement with experimental measurements. In this part of the series, we demonstrate the utility of the method on shocked liquid NO, where again, the agreement with laboratory measurements is excellent. The results show that the RxMC methodology provides a new simulation tool capable of testing models used in current detonation theory predictions. Further novel applications and extensions of the RxMC method are discussed.					
15. SUBJECT TERMS molecular simulation, Monte Carlo, Hugoniot, reaction ensemble					
16. SECURITY CLASSIFICATION OF:			17. LIMITATION OF ABSTRACT UL	18. NUMBER OF PAGES 22	19a. NAME OF RESPONSIBLE PERSON John K. Brennan
a. REPORT UNCLASSIFIED	b. ABSTRACT UNCLASSIFIED	c. THIS PAGE UNCLASSIFIED			19b. TELEPHONE NUMBER (Include area code) 410-306-0678

Contents

List of Figures	iv
List of Tables	iv
Acknowledgments	v
1. Introduction	1
2. Methodology	1
2.1 Reaction Ensemble Monte Carlo	1
2.2 Calculation of Shock Hugoniot Properties.....	2
3. Simulation Model and Details	2
3.1 Intermolecular Potential Models	2
3.2 Simulation Details	3
4. Application	3
5. Discussion	4
6. References	9
Distribution List	11

List of Figures

Figure 1. Shock Hugoniot of liquid NO. Calculated values from RxMC simulations (\circ) model are compared with experimental data (\blacktriangle) (11). The shock pressure is plotted vs. the specific volume.....	6
Figure 2. Shock Hugoniot of liquid NO. Calculated values from RxMC simulations (\circ) model are compared with experimental data (\blacktriangle) (11). The shock pressure is plotted vs. the shock wave velocity.	7
Figure 3. Species mole fractions (NO: [\blacklozenge]; either N_2 or O_2 [Δ]) along the Hugoniot curve determined from RxMC simulations of the NO decomposition reaction. Mole fractions plotted as “products” represent the values for both N_2 and O_2	8

List of Tables

Table 1. Exponential-6 potential parameters.	3
Table 2. Initial fluid states used to evaluate equation 2.	4
Table 3. Constant-pressure RxMC simulations of shocked liquid NO.....	5
Table 4. Shock Hugoniot states of liquid nitric oxide. Experimental data taken from Schott et al. (11).	6

Acknowledgments

The authors wish to thank Martin Lisal (Institute of Chemical Process Fundamentals, Academy of Sciences of the Czech Republic) for helpful discussions and critical reading of this manuscript prior to publication. This work was performed while John K. Brennan held a National Research Council Research Associateship Award at the U.S. Army Research Laboratory. The calculations reported in this work were performed at the U.S. Army Research Laboratory Major Shared Resource Center, Aberdeen Proving Ground, MD.

INTENTIONALLY LEFT BLANK.

1. Introduction

In the first report of this series, we introduced the Reaction Ensemble Monte Carlo (RxMC) method as a novel simulation tool for studying the behavior of materials under conditions of extreme temperature and pressure (*1*). The difficulties encountered in experimental measurements and theoretical predictions of these materials were delineated. Furthermore, a review of the limitations of currently available computational approaches illustrated the need for a simulation tool capable of more accurately predicting the shock properties of materials.

In this work, we demonstrate the applicability of the RxMC method for calculating the shock Hugoniot properties of liquid NO. Shocked liquid NO, which has been studied extensively by both experimental and theoretical techniques, is (nearly) an irreversible decomposition reaction that generates a mixture of the homonuclear products, N_2 and O_2 .

The outline of this report is as follows. A brief review of the RxMC methodology applied to the simulation of the shock properties of materials is given in section 2. Simulation details and models can be found in section 3, and application of the method to shocked liquid NO is presented in section 4. Finally, discussion of the results and possible extensions of the method are given in section 5.

2. Methodology

2.1 Reaction Ensemble Monte Carlo

The RxMC method (*2, 3*) is designed to minimize the Gibbs free-energy, thus determining the true chemical equilibrium state irrespective of rate limitations. RxMC requires intermolecular potentials for the molecular species that are present in the reactive mixture (*4*). RxMC also requires inputting the ideal-gas internal modes (vibration, rotation, and electronic) for each reactive species. These contributions can be included by calculating internal partition functions from molecular energy-level data (*2*) or by using tabulated thermochemical data (*3*). Regardless of the approach taken, the required information is readily available in standard sources (*4–6*) or can be generated using quantum mechanical calculations. Finally, the particular reactions occurring in the system must be specified.

Implementation of RxMC provides information on the chemical equilibrium state, such as the density of the reactive mixture, mole fractions of reactive species, the change in the total number of moles, and the internal energy. RxMC directly samples forward and reverse reaction steps as Monte Carlo-type moves according to the stoichiometry of the reactions being sampled. Further details of the RxMC method can be found in the first report of this series (*1*).

2.2 Calculation of Shock Hugoniot Properties

The thermodynamic quantities of a material in the initial unshocked state and the final shocked state are related by the conservation equations of mass, momentum, and energy across the shock front (7). The shock wave velocity D can be calculated from the Rayleigh line,

$$R = \rho_o^2 D^2 - (P - P_o)(V_o - V) = 0, \quad (1)$$

while the Hugoniot function satisfies the expression (7)

$$H_g(T, V) = 0 = E - E_o - \frac{1}{2}(P + P_o)(V_o - V). \quad (2)$$

In equations 1 and 2, E is the specific internal energy, P is the pressure, ρ is the specific density, $V=1/\rho$ is the specific volume, and D is the velocity of the shock wave propagating through the material, while the subscript “o” refers to the quantity in the initial unshocked state. Details of the search algorithm for locating a point on the Hugoniot curve used in this study can be found in the first report of this series (1).

3. Simulation Model and Details

3.1 Intermolecular Potential Models

The species particles interact through the exponential-6 potential, which can be expressed as

$$U_{\text{exp-6}}(r) = \begin{cases} \infty & r < r_{\text{core}} \\ \frac{\varepsilon}{1 - \frac{6}{\alpha}} \left[\frac{6}{\alpha} \exp\left(\alpha \left[1 - \frac{r}{r_m}\right]\right) - \left(\frac{r_m}{r}\right)^6 \right] & r \geq r_{\text{core}} \end{cases}, \quad (3)$$

where ε is the depth of the attractive well between particles, r_m is the radial distance at which the potential is a minimum, while α controls the steepness of the repulsive interaction. The cutoff distance r_{core} is included to avoid the unphysical singularity in the potential function as $r \rightarrow 0$. The potential parameters for the species considered in this work are given in table 1. A spherical cutoff for the particle-particle interactions was applied at $4.5r_{m,\text{NO}}$ without applying any correction for this truncation (8). Electrostatic contributions were ignored between species. The unlike interactions between species i and j were approximated by the Lorentz-Berthelot mixing rules (4) for ε_{ij} , α_{ij} , and $r_{m,ij}$:

$$\varepsilon_{ij} = (\varepsilon_i \varepsilon_j)^{1/2}; \quad \alpha_{ij} = (\alpha_i \alpha_j)^{1/2}; \quad r_{m,ij} = (r_{m,i} + r_{m,j})/2;$$

while

$$r_{\text{core},ij} = (r_{\text{core},i} + r_{\text{core},j})/2. \quad (4)$$

Table 1. Exponential-6 potential parameters.

Species	r_{core} (Å)	r_m (Å)	ϵ/k_B (K)	α	Source (Reference No.)
NO	1.00	3.995	117.1	12.08	(11)
N ₂	0.98	4.251	75.0	13.474	(11)
O ₂	0.96	4.110	75.0	13.117	(11)

The vibrational and rotational contributions to the ideal-gas partition functions used in simulating the NO decomposition reaction were calculated using a standard source (5) and supplemented with electronic level constants (6, 9).

3.2 Simulation Details

Constant-pressure RxMC simulations of shocked NO were initiated from 3375 NO particles, placed on a face-centered-cubic lattice structure. The standard periodic boundary conditions and minimum image convention were used (10). Simulations were performed in steps, where a step (chosen with equal probability) was either a particle displacement, forward reaction step, or reverse reaction step. A change in the simulation cell volume was attempted every 2500 steps. Simulations were equilibrated for 0.3×10^7 steps after which averages of the quantities were taken over 2.0×10^7 steps. Uncertainties were estimated using the method of block averages by dividing the production run into 10 equal blocks (8). Reported uncertainties are one standard deviation of the block averages. The maximum displacement and volume change were adjusted to achieve an acceptance fraction of ~ 0.33 and 0.5 , respectively. Depending on the system conditions, the acceptance fraction of the reaction steps ranged from 0.075 – 0.375 . Calculated quantities were reduced by the exponential-6 potential energy (ϵ) and size (r_m) NO parameters.

4. Application

We consider the decomposition of nitric oxide: $2\text{NO} \rightleftharpoons \text{N}_2 + \text{O}_2$. This reaction generates a mixture of homonuclear products that are miscible with each other and (assumed to be) with residual NO. The concentrations of other products such as NO_2 are considered to be negligible as are the accompanying reactions, e.g., $\frac{1}{2}\text{N}_2 + \text{O}_2 \rightleftharpoons \text{NO}_2$.

We determined the shock Hugoniot properties of liquid NO using the calculated initial conditions given in table 2. An NVT Monte Carlo simulation was performed for $N = 3375$ NO molecules at $T = 122.6$ K and at a specific volume of $V = 0.7905$ cm³/g. The calculated pressure and internal energy from this simulation are compared with experimental measurements in table 2. The shock Hugoniot properties were determined by the prescription outlined in section 2.2 of the first report of this series (1). The raw simulation data and the calculated quantities determined from a series of constant-pressure RxMC simulations at several different temperatures are given in table 3. Quadratic polynomials were used in the fitting procedure with

Table 2. Initial fluid states used to evaluate equation 2.

Thermodynamic Property	Liquid NO	
	Experiment (11)	NVT-MC
Temperature, T (K)	$122.6 + 2.3/-1.1$	122.6
Density, ρ (g/cm ³)	$1.263 + 0.06/-0.11$	1.265
Pressure, P (MPa)	—	490.5 ± 0.1
Energy, E (kJ/g)	2.650 ± 0.01	2.60 ± 0.01

the exception of the shock wave velocity (D) where a linear equation was used. A comparison of the shock properties along the principal Hugoniot calculated from the RxMC simulations and the experimental data of Schott and co-workers (11) is given in table 4. In table 4, an estimate of the uncertainties in the RxMC calculations of the shock Hugoniot properties can be determined from the R-square value of the functional fit of data given in table 3. Typical R-square values for the predicted temperatures and specific volumes are 0.97–0.99. Plots of the shock Hugoniot pressure vs. the specific volume and the shock wave velocity are given in figures 1 and 2, respectively. Again, excellent agreement between the RxMC calculations and the experimental measurements is found with typical differences of 1%–2%. Plots of the species mole fractions along the Hugoniot curve are shown in figure 3. Values of the mole fractions shown are interpolated from the data given in table 3 to T_{Hg} using a quadratic function. Since the mole fractions of N_2 and O_2 are equivalent, their mole fractions are plotted as “products” in figure 3. It is evident from figure 3 that as the pressure increases along the Hugoniot curve, the reaction equilibria shifts to an increasing amount of NO.

5. Discussion

We have demonstrated the effectiveness of using the RxMC simulation method for determining the shock properties of materials. We found the RxMC calculations to be in excellent agreement with the available experimental data for two simple systems. These demonstrations have illustrated the utility of the method for predicting the shock Hugoniot of mixtures for which species concentrations are not known and in the absence of interaction potentials that simulate bond breakage and formation.

Subsequent to the validation of the method presented in this report series, there are several possible extensions of the current RxMC methodology. First, although the computations are reasonably inexpensive, it may be possible to reformulate the method within other ensembles (e.g., constant-pressure, -enthalpy, and -number of particles [NPH]), allowing the calculation of the Hugoniot curve to be carried out more efficiently and conveniently (12). Further, the RxMC

Table 3. Constant-pressure RxMC simulations of shocked liquid NO.

T (K)	<P> (GPa)	Mole Fraction ^a			<V> (cm ³ /g)	<U ^{conf} > (kJ/g)	H ^o (kJ/g)	E (kJ/g)	H _g (kJ/g)	D (km/s)
		<x(N ₂)>	< x(O ₂)>	< x(NO)>						
P _{imp} = 14.47 GPa										
2250	14.483(1)	0.4791(1)	0.4791(1)	0.0419(1)	0.5077(5)	1.673(1)	2.3550	3.404	−1.310	5.560
2500	14.473(2)	0.4649(2)	0.4649(2)	0.0702(2)	0.5123(9)	1.688(2)	2.7543	3.750	−0.9286	5.604
2750	14.487(2)	0.4468(2)	0.4468(2)	0.1064(2)	0.5164(9)	1.705(1)	3.1788	4.122	−0.5282	5.649
3000	14.476(1)	0.4257(4)	0.4257(4)	0.1486(4)	0.5206(7)	1.718(1)	3.6234	4.510	−0.1068	5.690
3250	14.476(2)	0.4026(4)	0.4026(4)	0.1949(4)	0.5241(7)	1.729(1)	4.0819	4.910	0.3198	5.728
P _{imp} = 17.93 GPa										
2500	17.934(1)	0.4572(2)	0.4572(2)	0.0856(2)	0.4783(6)	2.042(1)	2.8008	4.150	−1.323	5.909
2750	17.965(2)	0.4366(2)	0.4366(2)	0.1268(2)	0.4812(9)	2.061(2)	3.2400	4.539	−0.9127	5.941
3000	17.921(1)	0.4135(4)	0.4135(4)	0.1730(4)	0.4842(7)	2.069(2)	3.6966	4.934	−0.4825	5.964
3250	17.927(2)	0.3885(4)	0.3885(4)	0.2229(4)	0.4866(7)	2.080(2)	4.1657	5.345	−0.0506	5.988
3275	17.946(2)	0.3859(6)	0.3859(6)	0.2283(6)	0.4868(7)	2.083(2)	4.2133	5.389	−0.0077	5.992
3300	17.944(3)	0.3833(4)	0.3833(4)	0.2333(4)	0.4870(9)	2.085(2)	4.2608	5.431	0.0369	5.995
P _{imp} = 21.03 GPa										
2700	21.036(2)	0.4314(4)	0.4314(4)	0.1372(4)	0.4565(5)	2.363(3)	3.2080	4.823	−1.369	6.200
2900	21.031(1)	0.4119(3)	0.4119(3)	0.1763(3)	0.4580(7)	2.370(2)	3.5790	5.146	−1.029	6.213
3100	21.035(2)	0.3911(5)	0.3911(5)	0.2178(5)	0.4596(7)	2.380(1)	3.9582	5.480	−0.6785	6.229
3300	21.054(3)	0.3697(5)	0.3697(5)	0.2606(5)	0.4609(9)	2.391(2)	4.3422	5.819	−0.3287	6.244
3400	21.061(1)	0.3592(4)	0.3592(4)	0.2815(4)	0.4614(8)	2.395(2)	4.5332	5.986	−0.1565	6.250
3500	21.031(2)	0.3489(5)	0.3489(5)	0.3021(5)	0.4623(5)	2.395(2)	4.7230	6.148	0.0207	6.254
P _{imp} = 25.47 GPa										
3000	25.487(2)	0.3830(8)	0.3830(8)	0.2339(8)	0.4301(14)	2.800(3)	3.8790	5.848	−1.430	6.584
3250	25.478(2)	0.3551(9)	0.3551(9)	0.2898(9)	0.4312(8)	2.809(2)	4.3654	6.274	−0.9874	6.593
3500	25.508(3)	0.3277(9)	0.3277(9)	0.3445(9)	0.4325(6)	2.826(2)	4.8494	6.706	−0.5450	6.608
3750	25.467(2)	0.3024(5)	0.3024(5)	0.3952(5)	0.4336(9)	2.828(3)	5.3212	7.110	−0.1177	6.613
4000	25.488(3)	0.2785(8)	0.2785(8)	0.4429(8)	0.4349(7)	2.843(2)	5.7857	7.520	0.3045	6.628
P _{imp} = 28.47 GPa										
3200	28.455(3)	0.3468(4)	0.3468(4)	0.3065(4)	0.4149(4)	3.080(2)	4.3514	6.545	−1.488	6.821
3400	28.477(2)	0.3241(7)	0.3241(7)	0.3518(7)	0.4155(7)	3.091(2)	4.7425	6.892	−1.136	6.829
3600	28.475(2)	0.3029(5)	0.3029(5)	0.3943(5)	0.4163(5)	3.101(2)	5.1259	7.229	−0.7869	6.836
3800	28.445(4)	0.2831(6)	0.2831(6)	0.4337(6)	0.4172(8)	3.107(3)	5.5004	7.555	−0.4434	6.840
4000	28.497(3)	0.2647(8)	0.2647(8)	0.4705(8)	0.4175(7)	3.116(2)	5.8672	7.875	−0.1271	6.850
4200	28.492(5)	0.2478(8)	0.2478(8)	0.5044(8)	0.4186(9)	3.127(3)	6.2255	8.189	0.2025	6.859

^aMole fraction of species i , $x(i) = N_i/N_{\text{total}}$, where N is the number of particles. $N_{\text{total}} = 3375$.

Table 4. Shock Hugoniot states of liquid nitric oxide. Experimental data taken from Schott et al. (11).

P (GPa)		V (cm ³ /g)		T (K)		D (km/s)		E (kJ/g)	
Exp.	RxMC ^a	Exp.	RxMC	Exp.	RxMC	Exp.	RxMC	Exp.	RxMC
14.47	14.47	0.5203	0.5215	—	3064.9	5.767	5.700	4.663	4.611
17.93	17.93	0.483	0.4868	—	3278.9	6.033	5.992	5.437	5.395
21.03	21.03	0.4627	0.4622	—	3488.2	6.337	6.255	6.087	6.132
25.47	25.47	0.437	0.4340	—	3819.1	6.715	6.619	7.157	7.227
28.47	28.47	0.4212	0.4180	—	4074.4	6.940	6.853	7.903	7.993

^aPressure imposed in the constant-pressure version of the RxMC method.

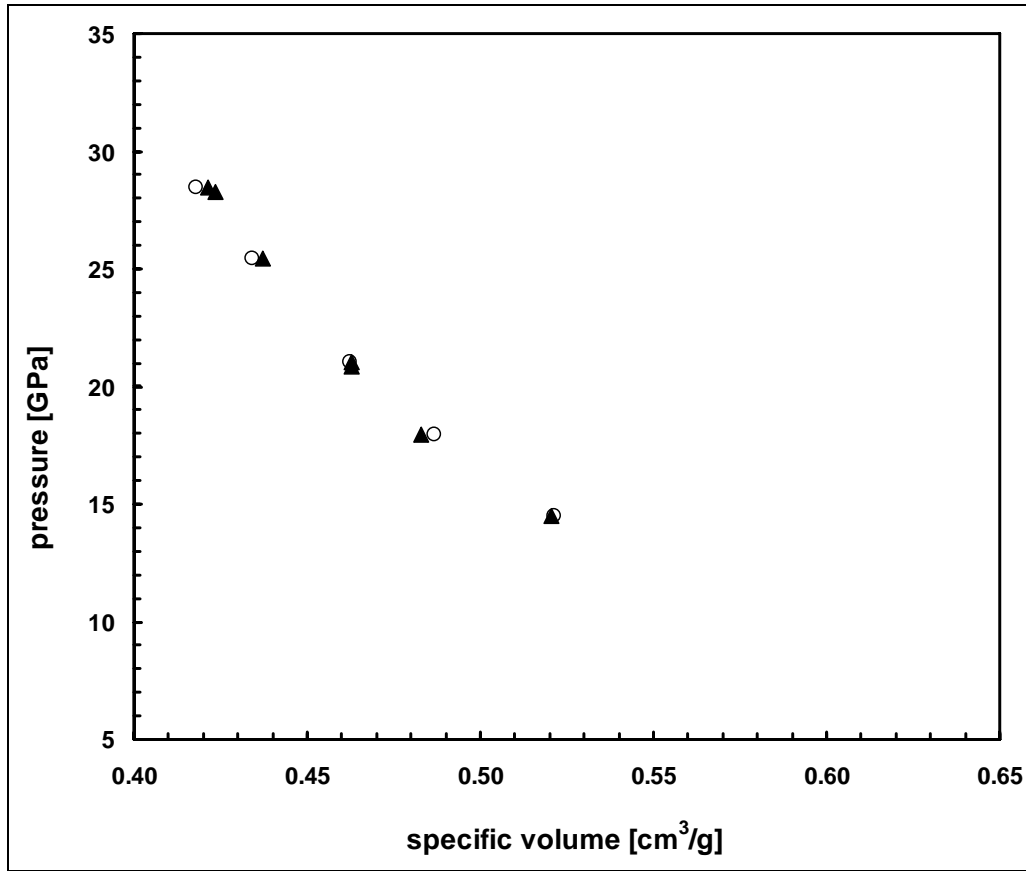


Figure 1. Shock Hugoniot of liquid NO. Calculated values from RxMC simulations (○) model are compared with experimental data (▲) (11). The shock pressure is plotted vs. the specific volume.

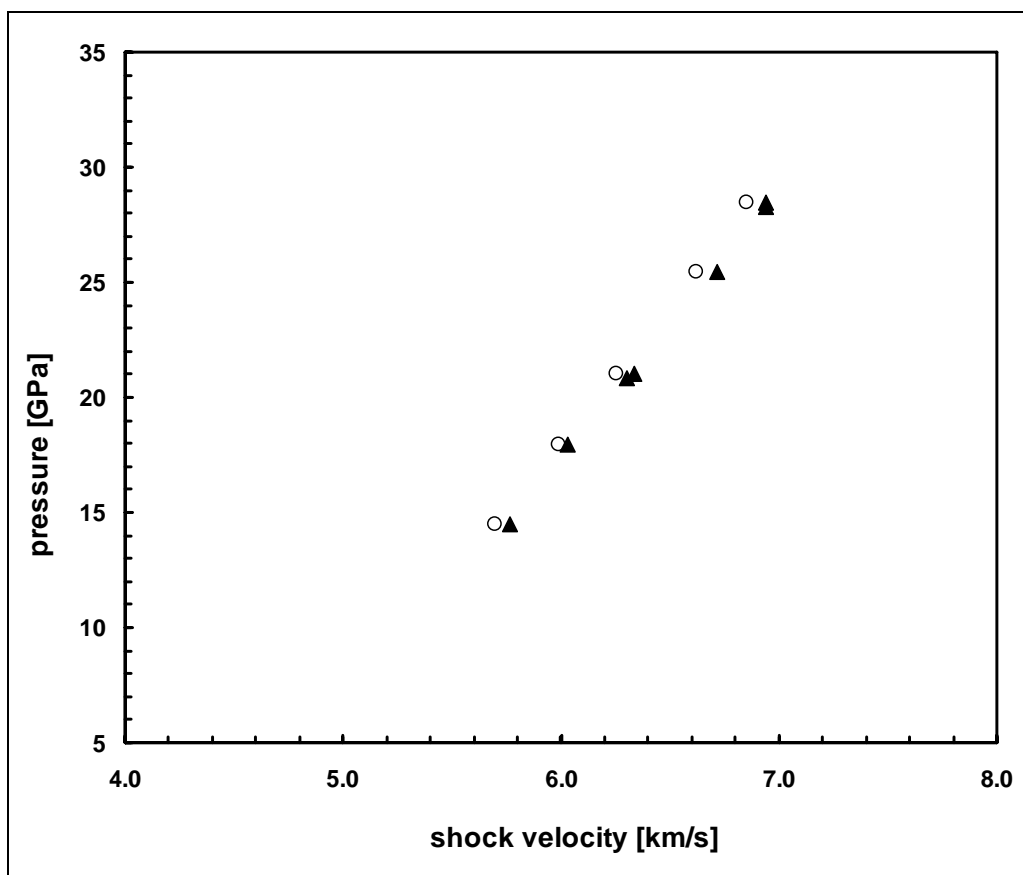


Figure 2. Shock Hugoniot of liquid NO. Calculated values from RxMC simulations (\circ) model are compared with experimental data (\blacktriangle) (11). The shock pressure is plotted vs. the shock wave velocity.

method has been recently combined with transition state theory to allow for the calculation of reaction rates (13). Thus, extension of the method to reaction rate calculations for materials under shock may also be possible.

A coordinated approach that links experimental, theoretical, and RxMC efforts appears promising in furthering our understanding of chemical reacting systems in highly nonideal environments. The RxMC method can perform several different functions in such approaches. First, RxMC can play a critical role in assessing theoretical models used in thermochemical codes. In these approaches, predictions using the model are usually obtained through approximate methods. Molecular simulation, on the other hand, provides an essentially exact result (within statistical uncertainty) for the model being considered and thus provides a means of testing these approximations. Furthermore, the underlying model of the theory can be tested by comparisons of simulation results to experiment.

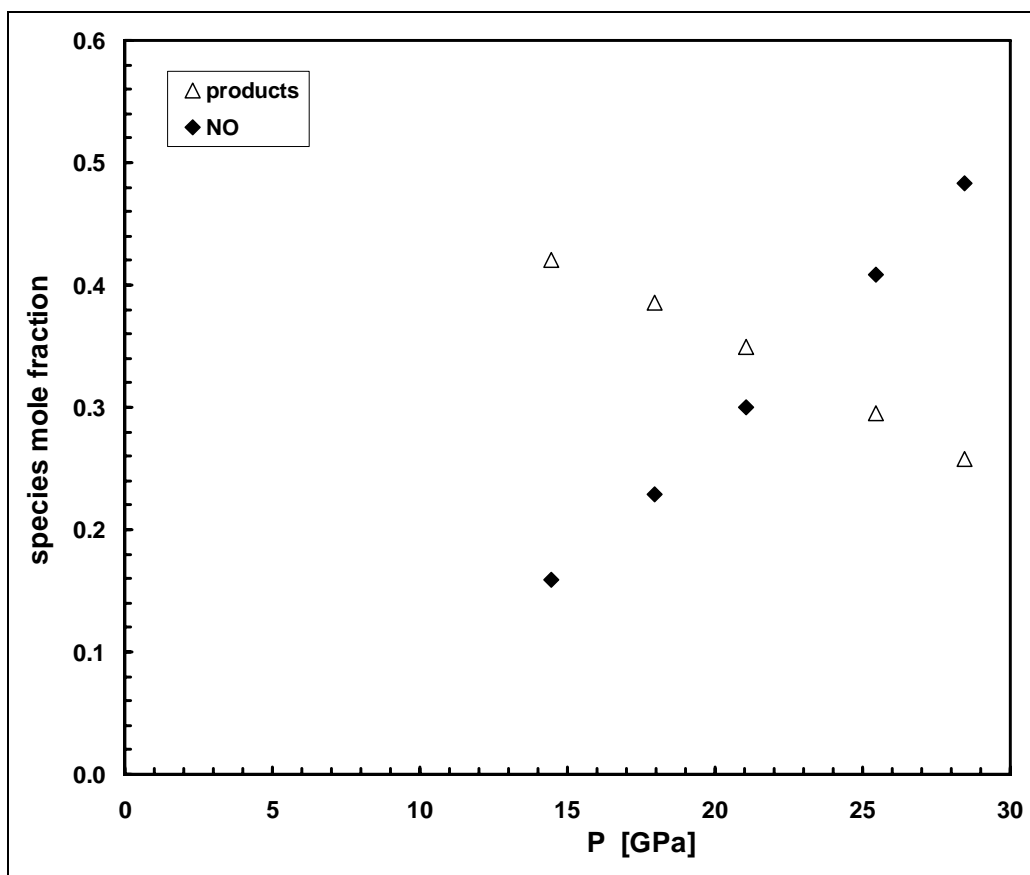


Figure 3. Species mole fractions (NO: [◆]; either N₂ or O₂ [Δ]) along the Hugoniot curve determined from RxMC simulations of the NO decomposition reaction. Mole fractions plotted as “products” represent the values for both N₂ and O₂.

The RxMC method can also be a powerful tool in the development of novel energetic materials. In lieu of the synthesis of a candidate material and the measurement of its thermophysical properties, quantum mechanical information can be generated to provide the ideal gas partition functions required for the simulation, while ab initio calculations can be used to parameterize the functions that describe the intermolecular interactions between the reactant and the species believed to exist in the product mixture. With these quantities in hand, RxMC can be used to predict shock properties of the notional material, thus providing crucial detonation performance information while avoiding costly and time-consuming experimental measurements.

RxMC can also be used to study the reactions of energetic materials in other nonideal environments, e.g., confined within polymer membranes, carbon nanotubes, or other porous materials, or for naval applications near or underwater. Finally, the RxMC method can be applied to the study of the supercritical phase separation behavior that theory suggests occurs for some detonation products (e.g., references [14–16]). Presently, this behavior has not been verified by experimental measurements. The RxMC method can be used to simulate multiple phase systems. Application of the method to such systems may provide further insight into this phenomenon.

6. References

1. Brennan, J. K.; Rice, B. M. Molecular Dynamics Simulations of SiO₂; U.S. Army Research Laboratory: Aberdeen Proving Ground, MD, in preparation, 2005.
2. Johnson, J. K.; Panagiotopoulos, A. Z.; Gubbins, K. E. Reactive Canonical Monte Carlo - A New Simulation Technique for Reacting or Associating Fluids. *Mol. Phys.* **1994**, *81*, 717.
3. Smith, W. R.; Tříska, B. The Reaction Ensemble Method for the Computer Simulation of Chemical and Phase Equilibria. I. Theory and Basic Examples. *J. Chem. Phys.* **1994**, *100*, 3019.
4. Reed, T. M.; Gubbins, K. E. *Applied Statistical Mechanics*; McGraw-Hill: New York, NY, 1973.
5. McQuarrie, D. A. *Statistical Mechanics*; Harper: New York, NY, **1976**.
6. Chase, M. W.; Davies, C. A.; Downey, J. R.; Frurip, D. J.; McDonald, R. A.; Syverud, A. N. JANAF Thermochemical Tables, Third Edition. *J. Phys. Chem. Ref. Data*, **1985**, *14*.
7. Fickett, W.; Davis, W. C. *Detonation*; University of California Press: Berkeley, CA, 1979.
8. Frenkel, D.; Smit, B. *Understanding Molecular Simulation*; Academic Press: San Diego, CA, 1996.
9. Huber, K. P.; Herzberg, G. *Molecular Spectra and Molecular Structure IV. Constants of Diatomic Molecules*; Van Nostrand Reinhold: New York, NY, 1979.
10. Allen, M. P.; Tildesley, D. J. *Computer Simulation of Liquids*; Oxford University Press: Oxford, U.K., 1987.
11. Schott, G. L.; Shaw, M. S.; Johnson, J. D. Shocked States from Initially Liquid Oxygen—Nitrogen Systems. *J. Chem. Phys.* **1985**, *82*, 4264.
12. Lísal, M.; Smith, W. R. Institute of Chemical Process Fundamentals, Academy of Sciences of the Czech Republic. Private communication, 2002.
13. Turner, C. H.; Brennan, J. K.; Johnson, J. K.; Gubbins, K. E. Effect of Confinement by Porous Materials on Chemical Reaction Kinetics. *J. Chem. Phys.* **2002**, *116*, 2138.
14. Ree, F. H. Supercritical Fluid Phase Separations: Implications for Detonation Properties of Condensed Explosives. *J. Chem. Phys.* **1986**, *84*, 5845.

15. Fried, L. E.; Howard, W. M. The Equation of State of Supercritical HF, HCl, and Reactive Supercritical Mixtures Containing the Elements H, C, F, and Cl. *J. Chem. Phys.* **1999**, *110*, 12023.
16. Ree, F. H.; Viecelli, J. A.; van Thiel, M. Influence of Fluorine Chemistry on Supercritical Fluid-Fluid Phase Separations. *J. Mol. Liq.* **2000**, *85*, 229.

NO. OF
COPIES ORGANIZATION

1 DEFENSE TECHNICAL
(PDF INFORMATION CTR
ONLY) DTIC OCA
8725 JOHN J KINGMAN RD
STE 0944
FORT BELVOIR VA 22060-6218

1 US ARMY RSRCH DEV &
ENGRG CMD
SYSTEMS OF SYSTEMS
INTEGRATION
AMSRD SS T
6000 6TH ST STE 100
FORT BELVOIR VA 22060-5608

1 DIRECTOR
US ARMY RESEARCH LAB
IMNE ALC IMS
2800 POWDER MILL RD
ADELPHI MD 20783-1197

3 DIRECTOR
US ARMY RESEARCH LAB
AMSRD ARL CI OK TL
2800 POWDER MILL RD
ADELPHI MD 20783-1197

ABERDEEN PROVING GROUND

1 DIR USARL
AMSRD ARL CI OK TP (BLDG 4600)

NO. OF
COPIES ORGANIZATION

1 DIRECTOR
US ARMY RESEARCH LAB
AMSRD ARL D
J MILLER
2800 POWDER MILL RD
ADELPHI MD 20783-1197

2 DIRECTOR
US ARMY RESEARCH LAB
AMSRD ARL RO P
R SHAW
TECH LIB
PO BOX 12211
RESEARCH TRIANGLE PARK NC
27709-2211

1 CDR US ARMY ARDEC
TECH LIB
PICATINNY ARSENAL NJ 07806-5000

1 CDR NAVAL RSRCH LAB
TECH LIBRARY
WASHINGTON DC 20375-5000

1 OFFICE OF NAVAL RSRCH
J GOLDWASSER
875 N RANDOLPH ST RM 653
ARLINGTON VA 22203-1768

1 CDR
NAVAL SURFACE WARFARE CTR
TECH LIB
INDIAN HEAD MD 20640-5000

1 CDR
NAVAL SURFACE WARFARE CTR
TECH LIB
DAHLGREN VA 22448-5000

1 AIR FORCE RSRCH LAB
MNME EN MAT BR
B WILSON
2306 PERIMETER RD
EGLIN AFB FL 32542-5910

1 AIR FORCE OFC OF SCI RSRCH
M BERMAN
875 N RANDOLPH ST
STE 235 RM 3112
ARLINGTON VA 22203-1768

NO. OF
COPIES ORGANIZATION

1 DIR SANDIA NATL LABS
M BAER DEPT 1512
PO BOX 5800
ALBUQUERQUE NM 87185

1 DIR LAWRENCE LIVERMORE NL
L FRIED
PO BOX 808
LIVERMORE CA 94550-0622

1 UNIV OF ALABAMA
DEPT OF CHEMICAL ENGRG
C TURNER
A132 BEVILL
TUSCALOOSA AL 35487-0286

ABERDEEN PROVING GROUND

61 DIR USARL
AMSRD ARL WM
T ROSENBERGER
AMSRD ARL WM M
S MCKNIGHT
AMSRD ARL WM T
B BURNS
AMSRD ARL WM TB
P BAKER
AMSRD ARL WM BD
R ANDERSON
W ANDERSON
R BEYER
A BRANT
G BROWN
S BUNTE
C CANDLAND
W CIEPIELA
G COOPER
L CHANG
T COFFEE
J COLBURN
P CONROY
B DAVIS
J DESPIRITO
N ELDREDGE
B FORCH
J GARNER
D HEPNER
B HOMAN
A HORST

NO. OF
COPIES ORGANIZATION

S HOWARD
P KASTE
G KATULKA
T KOGLER
A KOTLAR
C LEVERITT
R LIEB
D LYON
K MCNESBY
M MCQUAID
M MILLER
A MIZIOLEK
J MORRIS
J NEWBERRY
J NEWILL
M NUSCA (6 CPS)
W OBERLE
R PESCE-RODRIGUEZ
P PLOSTINS
S PIRIANO
G REEVES
B RICE
J SAHU
R SAUSA
S SILTON
E SCHMIDT
J SCHMIDT
P WEINACHT
D WILKERSON
A WILLIAMS
M ZOLTOSKI

NO. OF
COPIES ORGANIZATION

1 ACADEMY OF SCIENCES
OF THE CZECH REPUBLIC
E HALA LABORATORY
OF THERMODYNAMICS
M LISAL
165 02 PRAGUE 6-SUCHDOL
CZECH REPUBLIC